Available online at www.sciencedirect.com

ScienceDirect

Proceedings of the Combustion Institute 35 (2015) 617–624

Proceedings of the Combustion Institute

www.elsevier.com/locate/proci

Uncertainty analysis of the kinetic model prediction for high-pressure H_2/CO combustion

Xiaoyu Li [a,b], Xiaoqing You [a,b,*], Fujia Wu [c], Chung K. Law [a,c]

[a] Center for Combustion Energy, Tsinghua University, Beijing 100084, China

[b] Key Laboratory for Thermal Science and Power Engineering of Ministry of Education, Tsinghua University, Beijing 100084, China

[c] Department of Mechanical and Aerospace Engineering, Princeton University, Princeton, NJ 08544, USA

Available online 7 August 2014

Abstract

Recent studies showed that current H_2/CO kinetic models failed to match the measured laminar flame speeds of $H_2/O_2/CO_2$ mixtures at high pressures. To explore the source of discrepancy, we performed uncertainty analysis using the Data Collaboration method, and obtained dataset inconsistency if these measured values were included. We then conducted experiments at similar conditions and found that our new measured values are consistent with other data in the dataset. Our uncertainty analyses suggest two approaches to improve the model prediction performance: by reducing the uncertainties of model parameters directly, and by designing and conducting experiments that can effectively constrain the model predictions.

Keywords: H_2/CO combustion; Chemical kinetic model; Uncertainty analysis; Data Collaboration

1. Introduction

Synthetic gas (syngas), produced from gasification of coal and biomass and consisting mainly of H_2 and CO, is a potential fuel for future energy systems. The major challenge to utilizing syngas is how to achieve high efficiency and control emissions with its low heating value. An obvious solution to these problems lies in our understanding of the syngas combustion properties. Hence, it is essential to have a reliable chemical kinetics model to predict accurately the combustion of syngas and its emissions.

As a foundation of understanding the oxidation chemistry of hydrocarbon fuels, H_2/CO has been extensively studied (e.g. [1–5]). Although many efforts have been devoted to developing predictive H_2/CO oxidation models, a recent study showed that current models failed to predict the measured H_2 burning rate at high pressures [6]. As shown in Fig. 1, predictions of the models [3,7] deviate greatly from the measured mass burning rate [6] at elevated pressures. It is however not clear if the large discrepancies are due

* Corresponding author. Address: Center for Combustion Energy, and Department of Thermal Engineering, Tsinghua University, Beijing 100084, China. Tel.: +86 010 62771854.

E-mail address: xiaoqing.you@tsinghua.edu.cn (X. You).

http://dx.doi.org/10.1016/j.proci.2014.07.047

1540-7489/

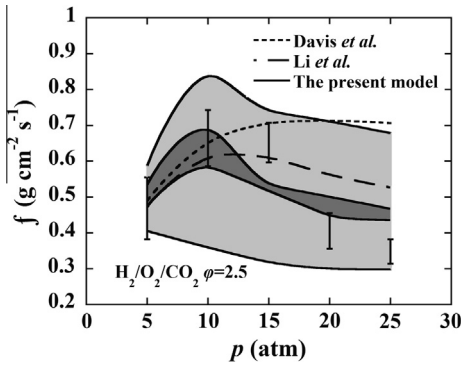

Fig. 1. Mass burning rate of $H_2/O_2/CO_2$ at $T_0 = 298$ K, $\varphi = 2.5$, $T_f = 1600$ K. Error bar: Burke et al. [6] Lines: modeling results; light gray: prediction uncertainties using dataset $D_l = \{ig1–6; flw1–3; fls1–9, 11, 12\}$; dark gray: prediction uncertainties using dataset $D_d = \{D_l; flw4–7; fls10'b, 10\}$.

to uncertainties in the model parameters or experimental measurements.

In this regard we first note that while model parameters have their own uncertainties, usually only representative values are taken in most computational modeling. As such, it is not uncommon to adjust values of the model parameters in order to improve the agreement between the model predictions and certain experimental results. This practice, however, overlooks the influence of adjusting parameters on predictions against other experiments, and consequently could lead to unreliable kinetic models. Therefore, in order to improve the model predictive ability, model parameters should be adjusted in a systematic manner on the basis of a wide range of experiments. The widely used model GRI-Mech 3.0 [8] for natural gas combustion, developed through validation and optimization against a large number of carefully chosen experimental targets, is a successful example of such a systematic approach. It is nevertheless noted that although this is an efficient and effective approach, model predictions being unconstrained by experimental target uncertainties, could fall out of the experimental error ranges [9].

In recent years, uncertainty analysis has become an important approach to improving kinetic model predictions, and several uncertainty analysis methods have been formulated [10–23]. In particular, Frenklach and coworkers [18–23] developed the method of Data Collaboration, using experimental uncertainties as constraints of model predictions, to check data-model consistency, make predictions, and optimize models on a feasible dataset. To facilitate the data analysis, You et al. [24] built a cyber-infrastructure to bridge the data infrastructure with Data Collaboration, and demonstrated its utility for the chemical kinetics of hydrogen combustion.

In this study, we performed quantitative uncertainty analysis of the H_2/CO kinetic model using Data Collaboration, and found that the dataset was inconsistent if the measured laminar flame speeds by Burke et al. [6] for $H_2/O_2/CO_2$ mixtures at 15, 20, 25 atm were included. We then evaluated two approaches to improve the model prediction; one by changing the uncertainty bounds of the model parameters, and the other through designing experiments that can effectively constrain the model predictions. Our objective is to minimize the prediction uncertainty of the H_2/CO model, and to resolve the inconsistency caused by measured laminar flame speeds at elevated pressures [6]. To scrutinize our uncertainty analysis, we further conducted experiments at similar conditions as those of Burke et al. [6], and found that our measured values are indeed consistent with the other data in the dataset, hence substantiating the viability of the present approach.

This article is organized as follows. First, we describe the Data Collaboration method and the experimental method briefly, and then introduce our as-compiled H_2/CO model, and the chosen experimental targets. Next, we discuss the H_2/CO dataset creation, consistency tests, uncertainty analyses, and experimental results.

2. Data Collaboration method

Data Collaboration is a method that assembles model parameters, experimental data and model predictions into a dataset. The uncertainties of the model parameters and experimental data are assumed to be uniformly distributed between the corresponding upper and lower bounds. The dataset $\mathbf{D}$ is a collection of dataset units D_e, and each dataset unit consists of the experimental value d_e, uncertainty lower and upper bounds l_e and u_e, and the model prediction $M_e(\mathbf{x}_e)$, shown as Eq. (1),

$$\mathbf{D} = \{D_e, 1 \leqslant e \leqslant m\} \quad \text{where}$$
$$D_e = \{d_e, l_e, u_e, M_e(\mathbf{x}_e)\} \tag{1}$$

where $M_e(\mathbf{x}_e)$ is a surrogate model in the form of quadratic functions, and is developed to represent model predictions by Solution Mapping—approximation of model responses via computer experiments and regression [25]. $\mathbf{x}_e$ is an active variable, and the union set of active variables of all dataset units is $\mathbf{x}$. The model prediction $M_e(\mathbf{x}_e)$ is constrained by the inequality,

$$l_e \leqslant M_e(\mathbf{x}_e) - d_e \leqslant u_e \quad \text{for } e = 1, \ldots, m \tag{2}$$

and the model parameters x_i is constrained by its lower and upper bounds $x_{i,\min}$ and $x_{i,\max}$,

$$x_{i,\min} \leqslant x_i \leqslant x_{i,\max} \quad \text{for } i = 1, \ldots, n \tag{3}$$

The subset of the parameter space that satisfies inequalities (2) and (3) for all dataset units is referred to as a feasible set, F. If F is nonempty,

the dataset is consistent; otherwise, it is inconsistent.

In addition, uncertainty sensitivity analysis [23] was used to estimate the effect on the prediction interval from the uncertainties of model parameters and experiments. The obtained sensitivity coefficients show which model parameters or experiments contribute the most to the uncertainty in the model prediction, and thereby provide guidance to experimental or theoretical research. Since the smaller experimental uncertainties have a stronger constraint on the model parameter uncertainties, we need accurate experimental facilities and methods.

3. Experimental method and considerations

Flame speeds in this study were measured in a dual-chamber high-pressure vessel. Detailed description of the vessel and methodology is given in Refs. [26,27], although it is necessary to also mention some specific details with the present experimentation because of the demand for enhanced certainty and accuracy. The apparatus consists of an inner chamber situated within an outer chamber of substantially larger volume. The inner chamber is filled with the test fuel/oxidizer mixture while the outer chamber is filled with a mixture of inert gases to match the density of the gas in the inner chamber. The two chambers are initially separated, and are mechanically connected at the instant of spark ignition such that the resulting flame would propagate in essentially an isobaric environment, and is quenched upon contacting the inert gas in the outer chamber before any substantial pressure builds up. The most important advantage of this dual-chamber design is that it allows constant-pressure flame speed measurement at high pressures.

Uncertainty of flame speed measurement using spherical flames can come from various sources, such as extrapolation of stretched flame speed to zero stretch, radiation of burned gas, mixture composition, etc. The uncertainty associated with radiation at conditions measured in this study (fls10a–10d in Table 2) was reported to be as small as 2% in the recent computations by Santner et al. [28] using the optically thin assumption (the most conservative estimate). Since the experimental conditions are at higher pressures, the flame thickness and thus thermal-diffusive effects are considerably smaller. Therefore, the uncertainty associated with stretch extrapolation is also smaller. Values of the parameter, $2L_b/R_{f,mid}$ (where L_b is the Markstein length, $R_{f,mid}$ is the averaged flame radius used for extrapolation [29]), for conditions measured in this study (fls10a–10d in Table 2) vary from 0.014 to 0.034, which are well within the range $-0.05 < 2L_b/R_{f,mid} < 0.15$ where the extrapolation uncertainty is small as shown by the computations in [29]. The mixture composition error during preparation of a high-pressure gas mixture is the largest source of uncertainty. In the present experiments, each condition was repeated 3–9 times and the repeatability is ±5%, which is caused by the mixture composition variation during the preparation of each mixture. We also found that if the combustion chamber is not flushed with new gases for enough time, the result of the next experiment will be affected because the combustion products from the last experiment (such as H_2O) may stick on the wall. In addition, when a gas is delivered from tank to the high-pressure chamber, it requires longer time to reach the equilibrium pressure. This can lead to an error in the mixture composition if enough time is not given during the filling process. In the present experiments, we have ensured that enough time was given in both the vacuuming and gas filling processes. Finally, the pressure gauges have a ±0.25% uncertainty, which in the worst scenario, e.g., when the reading for H_2 is −0.25% while that for O_2 is +0.25%, can cause an approximately 10% uncertainty in the flame speed. However, since the pressure gauges for all gases are calibrated against each other with linearity less than 0.03% (which causes less than 2% error in the flame speed), the worst scenario is not possible to occur. A ±0.25% error in the total pressure only causes 0.5% error in the flame speed. Therefore the uncertainty of flame speeds for the conditions considered in the present study is estimated to be ±5%.

4. Kinetic modeling of H_2/CO combustion

A large number of H_2/CO kinetic models (e.g. [3,4,7,30]) have been developed and validated against experimental data. In this study, we shall focus on the uncertainties of parameters rather than the specific values. Based on these studies, we collected the experimental data and evaluated the thermochemical and rate parameters, and compiled a detailed H_2/CO chemical kinetics model consisting of 14 species and 31 reactions. The rate parameters A, n, E_a, and bounds of A are shown in Table S1. The thermochemical data and transport data of the species were taken from You et al. [24] and Davis et al. [3], which incorporated the most recent updates from Burcat and Ruscic [31]. The H_2 submodel is also taken from You et al. [24], in which several rate parameters were updated and reasonable uncertainties were estimated based on extensive literature data. We took the 10-reaction CO submodel (listed in Table 1) from Davis et al. [3], except that the rate parameters of the reactions $CO + HO_2 = CO_2 + OH$ and $CO + OH = CO_2 + H$ were taken from two high-level theoretical studies by You et al. [32] and Joshi and Wang [33], respectively.

The other important ingredients of a dataset are experimental targets and their corresponding uncertainties. We took the shock tube ignition delays and flow reactor data of H_2 combustion that were considered as targets in You et al. [24]. In addition, we collected the H_2/CO data from [3,6] and this work, especially the laminar flame speeds at elevated pressures; our added targets are listed in Table 2.

The ignition delay times and flow reactor results were simulated by assuming adiabatic constant volume and adiabatic constant pressure condition, respectively. The sensitivity analyses for both were efficiently accomplished by using saturated factorial designs and Hadamard matrices, whose elements are either +1 or −1 and whose columns are mutually orthogonal [34]. Laminar flame speeds and the associated sensitivity coefficients with respect to the reaction rate constants and the binary mass diffusion coefficients were calculated using the PREMIX program [35], allowing for the effects of thermal diffusion and multicomponent transport.

5. H_2/CO dataset

5.1. Creating the H_2/CO dataset

We created the H_2/CO datasets from the as-compiled kinetic model of H_2/CO combustion (listed in Table S1) and experimental targets (listed in Table S2). We first identified active model parameters through sensitivity analyses, which rank the influence of pre-exponential factors of the rate coefficients on each prediction against the corresponding experimental target. For each target, the pre-exponential A factors of the reactions that show the 10–20 largest sensitivities on the prediction were chosen as the active parameters. To increase the numerical efficiency, surrogate models in the form of quadratic functions were developed to represent model predictions by Solution Mapping—approximation of the model responses via computer experiments and regression [20,25,36]. The surrogate models were built on the fly [24], similar to the sensitivity analysis, by performing a series of computational runs according to a design matrix [25]. The design was made using space-filling sampling by Latin hypercube designs [37]. The values of the responses, computed with the "full" chemical model, were fitted into a quadratic in active variables. The fitting error was minimized by increasing the number of design points, adjusting slightly the number of active parameters for the target, and repeating the design-regression process until the error is negligible. The coefficients of the surrogate models were stored appropriately so that they can be retrieved in the data analysis.

Our initial H_2/CO dataset includes 35 experimental targets (ig1–6; flw1–7; fls1–10', 11, 12 in Table S2), a total of 25 active parameters, and 35 surrogate models.

5.2. Testing consistence of dataset

After the dataset was created, consistency test was performed to check if there exists at least one set of the model parameter values within their respective ranges of uncertainties such that the surrogate model is able to predict the corresponding experimental targets within their respective ranges of uncertainties.

It turns out that the H_2/CO dataset is inconsistent. The laminar flame speeds for the $H_2/O_2/CO_2$ flames at pressures of 15, 20, 25 atm, marked by fls10'c, 10'd, 10'e (listed in Table 2), were found to be internally inconsistent, which implies that the present model cannot predict simultaneously the three targets well. Figure S1 shows the consis-

Table 1
CO submodel and the uncertainties of the pre-exponential factors ($AT^n e^{-Ea/RT}$, units: cm^3, mol, s, cal, K).

	Reactions	A	n	E_a	$[A_{lb}\ A_{ub}]/A$[a]	A_{opt}/A[a]	Ref.
22[b]	$CO + O + M = CO_2 + M$	1.17×10^{24}	−2.79	4191	[0.66 2.64]	0.6600	[3]
	$CO + O = CO_2$	1.36×10^{10}	0.00	2384			
23	$CO + OH = CO_2 + H$	7.05×10^{4}	2.05	−356	[0.50 2.00]	1.3356	[33]
	$CO + OH = CO_2 + H$	5.76×10^{12}	−0.664	332			
24	$CO + O_2 = CO_2 + O$	1.12×10^{12}	0.00	47,700	[0.84 6.78]	1.0000	[3]
25	$CO + HO_2 = CO_2 + OH$	1.57×10^{5}	2.18	17,943	[0.50 2.00]	1.0000	[32]
26	$HCO + H = CO + H_2$	1.20×10^{14}	0.00	0	[0.50 2.00]	1.8414	[3]
27	$HCO + O = CO + OH$	3.00×10^{13}	0.00	0	[0.50 2.00]	1.0000	[3]
28	$HCO + O = CO_2 + H$	3.00×10^{13}	0.00	0	[0.50 2.00]	1.0000	[3]
29	$HCO + OH = CO + H_2O$	3.02×10^{13}	0.00	0	[0.50 2.00]	1.0000	[3]
30[c]	$HCO + M = CO + H + M$	1.87×10^{17}	−1.00	17,000	[0.50 2.00]	1.0000	[3]
31	$HCO + O_2 = CO + HO_2$	1.20×10^{10}	0.81	−727	[0.19 1.69]	1.0000	[3]

[a] A_{lb} and A_{ub} are the lower and upper limits of A, respectively; A_{opt} are the optimized pre-exponential factors.
[b] Efficiency factors: $H_2 = 2.0$; $H_2O = 12.0$; $CO = 1.75$; $CO_2 = 3.6$; $Ar = 0.7$; $He = 0.7$.
[c] Efficiency factors: $H_2 = 2.0$; $CO = 1.75$; $CO_2 = 3.6$; $H_2O = 12.0$.

Table 2
Experimental targets and model predictions.

Exp. no.	Composition (% mol)				φ	T_f[a]	T_0	P	d	d_l[b]	d_u[b]	M_l[b]	M_d[b]	M_{opt}[b]	Ref.
	H_2	CO	O_2	Diluent		(K)	(K)	(atm)							
	Ignition delay time, ig						T_5	p_5	us						
6a[c]	0.05	12.17	1.00	Ar	6.09	–	2160	1.492	63	23	120	87	123	123	[3]
6b[c]	0.05	12.17	1.00	Ar	6.09	–	2625	1.949	23	7	47	14	47	33	[3]
	Flow reactor, flw						T_0	p_0	ppm/ms						
5[d]	–	1.014	0.517	N_2	1	–	1038	1	354	274	434	300	434	428	[3]
6[d]	–	0.988	0.494	N_2	1	–	1038	3.46	140	100	180	100	180	133	[3]
7[d]	–	1.002	0.482	N_2	1	–	1068	6.5	14	13	15	13	15	15	[3]
	Flame speed, fls						T_0	p	cm/s						
1	29.60	–	14.80	N_2	1	–	298	1	204	164	244	181	231	203	[3]
2	20.00	–	10.00	He	1	–	298	1	206	166	246	203	244	228	[3]
3	13.80	–	6.90	He	1	–	298	15	58	46	70	56	69	64	[3]
4	21.90	–	6.30	He	1.75	–	298	15	88	76	106	79	94	84	[3]
5	11.97	–	7.04	He	0.85	1600	298	25	15.6	14.2	16.7	14.2	16.7	16.7	[6]
6	11.83	–	5.92	He	1	1600	298	25	15.1	13.9	16.1	13.9	16.1	15.7	[6]
7a	32.21	–	6.44	Ar	2.5	1600	298	15	54.8	47.9	62.4	47.9	51.0	47.9	[6]
7b	32.21	–	6.44	Ar	2.5	1600	298	20	40.0	35.5	44.0	36.9	39.5	37.5	[6]
7c	32.21	–	6.44	Ar	2.5	1600	298	25	28.2	25.5	30.8	28.9	30.8	29.9	[6]
8	29.41	–	5.88	Ar	2.5	1500	298	20	20.0	17.0	22.5	19.8	22.0	20.7	[6]
9	35.21	–	7.04	Ar	2.5	1700	298	20	64.5	58.8	69.7	59.0	64.5	60.2	[6]
10'a	54.95	–	10.99	CO_2	2.5	1600	298	5	118.3	95.9	139.3	–	–	–	[6]
10'b	54.95	–	10.99	CO_2	2.5	1600	298	10	84.1	73.6	93.3	73.6	86.8	73.6	[6]
10'c	54.95	–	10.99	CO_2	2.5	1600	298	15	54.8	49.9	59.1	–	–	–	[6]
10'd	54.95	–	10.99	CO_2	2.5	1600	298	20	25.6	22.3	28.6	–	–	–	[6]
10'e	54.95	–	10.99	CO_2	2.5	1600	298	25	17.6	15.8	19.2	–	–	–	[6]
10a	53.54	–	10.71	CO_2	2.5	1620	353	5	153.1	145.4	160.7	145.4	160.7	147.0	This work
10b	53.54	–	10.71	CO_2	2.5	1616	353	15	55.0	52.3	57.8	52.3	53.3	52.3	This work
10c	53.54	–	10.71	CO_2	2.5	1632	353	20	33.2	31.5	34.9	34.1	34.9	34.9	This work
10d	53.54	–	10.71	CO_2	2.5	1632	353	25	25.4	24.1	26.6	24.9	26.6	25.6	This work
11a	15.57	15.57	6.23	Ar	2.5	1600	298	20	16.4	14.5	18.7	14.5	17.2	14.6	[6]
11b	15.57	15.57	6.23	Ar	2.5	1600	298	25	12.2	6.0	18.4	11.3	13.6	11.6	[6]
12	2.95	26.55	5.90	Ar	2.5	1600	298	20	7.6	6.6	8.5	7.2	8.5	8.5	[6]

[a] T_f: flame temperature.
[b] d_l, d_u: lower and upper bound of experiments, respectively; M_l, M_u: lower and upper bound of predictions, respectively; M_{opt}: optimal H_2/CO model predictions.
[c] Ignition delays of targets 6a and 6b are defined by maximum $d[CO_2]/dt$.
[d] Fuel composition includes 0.65% H_2O, and target value is $\Delta x_{CO}/\Delta t|_{C_{CO}=0.4}^{C_{CO}=0.6}$.

tency relationship among data. Among all data from Burke et al. [6], only fls10'c, 10'd, 10'e are inconsistent with other data in the dataset. Since the consistency analysis did not the consider the influence of the uncertainties of the transport parameters on the predicted H_2/CO flame speeds, the normalized sensitivity coefficients of $H_2/O_2/CO_2$ laminar flame speeds at pressures from 1 to 25 atm with respect to binary mass diffusion coefficients were calculated and shown in Fig. S2. It was found that the flame speeds at the pressures from 5 to 25 atm were affected by the same set of dominant transport coefficients (H_2–CO_2, O_2–CO_2, O_2–H_2O binary mass diffusion coefficients) with almost the same magnitude of sensitivity. Therefore, the flame speeds at high pressures can hardly achieve consistency through adjusting the values of the transport coefficients. On the other hand, from our sensitivity analysis on the consistency, we found that there are two possible kinetic causes for such a discrepancy, namely: (1) flame speeds measured at higher pressures may deviate from the ideal laminar flame speeds, especially when CO_2 is used as the diluent, (2) the rate parameters of several reactions, such as $2H(+M) = H_2(+M)$, $CO + O(+M) = CO_2(+M)$, may need to be studied further, as the kinetics of the third-body reactions are complex, especially when CO_2 is the third body.

To verify the above speculation, we measured the laminar flame speeds for $H_2/O_2/CO_2$ flames at 5–25 atm, which are marked as fls10a–10d in Table 2. Our experimental condition differs from that of Burke et al. [6] by mild variation of the mixture composition and a slightly higher initial temperature, at 353 K. From uncertainty analysis

(shown in Fig. S1), the new data at 15, 20, 25 atm are consistent with other data in Table S2, except for fls10'c, 10'd, 10'e from Burke et al. [6]. Assuming the uncertainties of these data are reasonably estimated, we believe our measurements are close to the proper laminar flame speeds.

We have therefore substituted the laminar flame speeds of $H_2/O_2/CO_2$ mixtures by Burke et al. [6] at pressures of 5, 15, 20, 25 atm (fls10'a, c–e) by the current measured data (fls10), as well as the rest of the dataset units to make predictions at various conditions, and conducted further uncertainty analyses.

Our predicted laminar flame speeds of $H_2/O_2/CO_2$ at pressures of 5–25 atm are shown in Fig. 1. Before being constrained by our experimental data, the model prediction uncertainties are large, colored in light gray. After our data were included in the dataset, the prediction uncertainties were largely reduced, colored in dark gray. It is noted that the prediction uncertainties at 15, 20, 25 atm have no intersection with the experiments by Burke et al. [6], which verifies the inconsistency of the two sets of data.

6. Uncertainty analysis of the H_2/CO model

6.1. Model parameter uncertainty

We first explore how model prediction uncertainties change with reduced model parameter uncertainties. We assembled datasets with experimental targets that are insensitive with respect to predictions and kinetic models with variable rate parameter uncertainties. We analyzed sensitivity of the predicted interval for high-pressure flame speeds with respect to the model parameter uncertainties and experiment uncertainties, respectively, as shown in Fig. 2. The uncertainties of the model predictions at given conditions usually do exhibit dependence on only a part of the model parameters and experimental targets. Figure 2a indicates four common rate parameters of reactions that have large sensitivities: $2H\ (+M) = H_2\ (+M)$ (R5), $H + O_2\ (+M) = HO_2\ (+M)$ (R9), $CO + O\ (+M) = CO_2\ (+M)$ (R22), $OH + CO = H + CO_2$ (R23). We built three datasets, D_{100}, D_{60}, D_{30}, including the common insensitive experiments: ig1–6; flw1–3; fls1–9. D_{100} includes the H_2/CO model with the trial model parameter uncertainties (listed in Table S1). For D_{60} and D_{30}, uncertainties for four common rate parameters of reactions R5, R9, R22, R23 are reduced to be 60% and 30% of the original parameter uncertainties, respectively.

We predicted the laminar flame speeds of $H_2/O_2/CO_2$ mixtures of equivalence ratio 2.5 at elevated pressures and an initial temperature of 353 K, and obtained variable prediction uncertainties as parameter uncertainties are reduced, as shown in Fig. 3. As expected, the prediction uncertainties of flame speeds at high pressures diminish as model parameter uncertainties are reduced. However, a subset of predictions is still outside the experimental uncertainties, even if

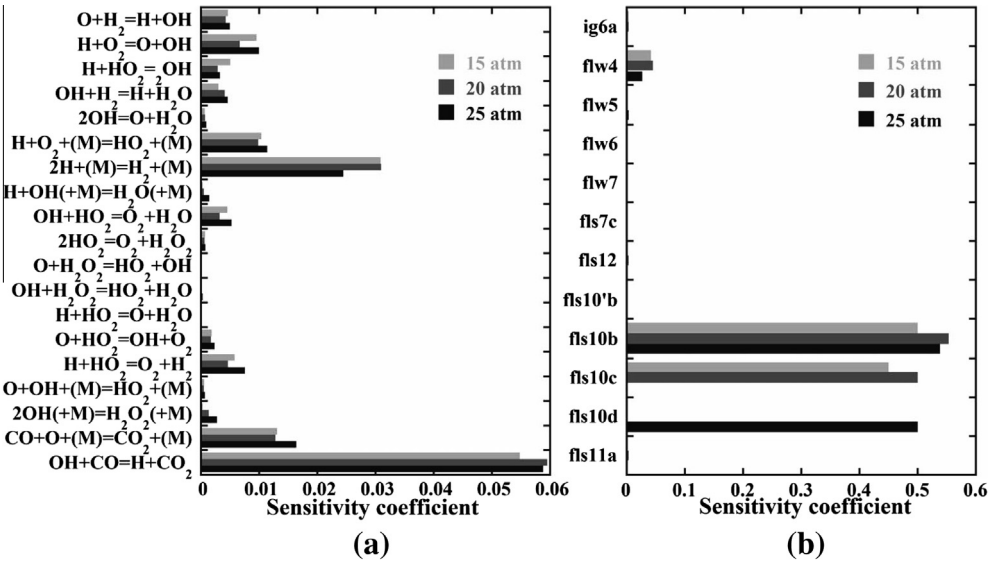

Fig. 2. Sensitivity coefficients of the prediction interval fls10b–d (in Table 2) with respect to the uncertainties in the model parameters (a) and targets (b), based on dataset D_a = {ig1–6; flw1–3; fls1–9} and D_b = {ig1–6; flw1–7; fls1–9, 10'b, 10–12} respectively.

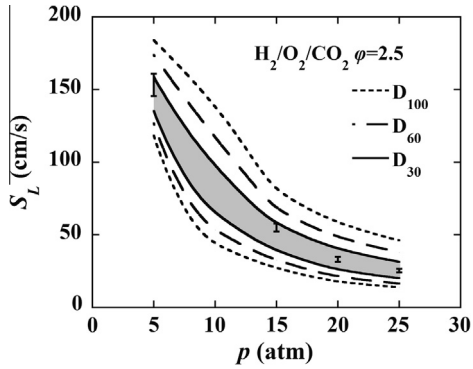

Fig. 3. Laminar flame speed of $H_2/O_2/CO_2$ at $T_0 = 353$ K, $\varphi = 2.5$, $T_f = 1600$ K. Error bar: this study; Lines: modeling prediction uncertainties.

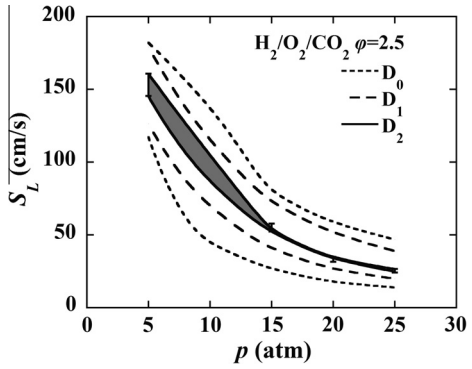

Fig. 4. Laminar flame speed of $H_2/O_2/CO_2$ at $T_0 = 353$ K, $\varphi = 2.5$, $T_f = 1600$ K. Error bar: this study; Lines: modeling prediction uncertainties. $D_0 = \{ig1–6; flw1–3; fls1–9\}$, $D_1 = \{D_0; flw4–7; fls10'b, 11–12\}$, $D_2 = \{D_1; fls10\}$.

the model parameter uncertainties are reduced to 30% of the original uncertainties.

We also explored the effects of parameter uncertainties after being constrained by experiments that show large sensitivities. Even though the rate parameter uncertainties are reduced to 50% of the original uncertainties, the prediction uncertainties scarcely diminish. Because a compact feasible set is generated after being constrained by experiments, it is difficult to further reduce model prediction uncertainties through reducing the parameter errors.

6.2. Experimental uncertainty

We next explore how model prediction uncertainties can be reduced through the constraints by experimental target uncertainties. As mentioned earlier, the uncertainties of model predictions at elevated pressures do exhibit dependence on only a part of the experimental targets, whose effects are ranked and shown in Fig. 2b as an example.

We chose three datasets, and predicted the laminar flame speeds of $H_2/O_2/CO_2$ at elevated pressures, as shown in Fig. 4. Here D_0 includes experiments that have small influence on their prediction uncertainty, D_1 consists of D_0 and experiments with moderate effect, and D_2 is formed through adding fls10, which have the largest effect, to D_1. From Fig. 4, the H_2/CO model prediction uncertainties of flame speeds at elevated pressures diminish, as experiments that constrain the feasible set are added to the dataset. Furthermore, the model prediction uncertainties reduce sharply after the flame speeds of $H_2/O_2/CO_2$ at 5–25 atm (fls10) are added, which is due to the common dominant reaction rates and small experimental uncertainties.

Furthermore, we predicted uncertainties on laminar flame speeds as the equivalence ratio and CO fraction in the fuel change, as shown in Figs. S3 and S4, respectively. They also provide guidance to the measurement strategy of laminar flame speeds at the associated conditions. Those experiments, whose uncertainties have an intersection with their predicted interval, may improve the H_2/CO model prediction performance.

6.3. Model optimization

Finally, we optimized the H_2/CO model by changing a minimal set of parameters within their own uncertainties, while keeping optimal model predictions within the uncertainty bounds of the corresponding experimental targets using the 1N-F optimization method described in [9]. The ratio of the optimized to the original A factors (A_{opt}/A) and the optimal model predictions are shown in Tables S1 and S2, respectively. The optimized kinetic model, the thermochemical data and transport data in CHEMKIN format were also provided in the supplemental material. It is found that 18 model parameters were changed within their own uncertainties, while keeping 35 model predictions fall within their corresponding experimental uncertainties.

7. Summary

In this study, we performed quantitative uncertainty analysis of the H_2/CO kinetic model using the Data Collaboration method. We found dataset inconsistency when a set of literature experimental laminar flame speeds for $H_2/O_2/CO_2$ mixture at 15–25 atm were included in the dataset. We then conducted experiments at similar conditions and found our new data to be consistent with the rest in the dataset. We further evaluated two approaches to improve the model prediction performance: by reducing the uncertainty bounds

of model parameters directly and by constraining the model predictions using experimental target uncertainties. Assisted by uncertainty sensitivity analysis, we are able to identify the model parameters or experiments that contribute the most to the prediction uncertainty. The experiments that have small uncertainties and common dominant reaction rates lead to a feasible set with reduced uncertainty. Consequently, we now not only have more trustworthy laminar flame speeds for H_2/CO combustion at elevated pressures, but have also demonstrated that our uncertainty analysis can successfully provide guidance to the measurement strategy of laminar flame speeds.

Acknowledgments

The work conducted at Tsinghua University was supported by the National Science Foundation of China (51206090), the National Basic Research Program (2013CB228502), and the 111 project (B13001).

Appendix A. Supplementary material

Supplementary data associated with this article can be found, in the online version, at http://dx.doi.org/10.1016/j.proci.2014.07.047.

References

[1] M. Chaos, F.L. Dryer, *Combust. Sci. Technol.* 180 (6) (2008) 1053–1096.
[2] A.M. Starik, N.S. Titova, A.S. Sharipov, et al., *Combust. Explos. Shock Waves* 46 (5) (2010) 491–506.
[3] S.G. Davis, A.V. Joshi, H. Wang, et al., *Proc. Combust. Inst.* 30 (1) (2005) 1283–1292.
[4] M.P. Burke, M. Chaos, Y. Ju, et al., *Int. J. Chem. Kinet.* 44 (7) (2012) 444–474.
[5] A. Frassoldati, T. Faravelli, E. Ranzi, *Int. J. Hydrogen Energy* 32 (15) (2007) 3471–3485.
[6] M.P. Burke, M. Chaos, F.L. Dryer, et al., *Combust. Flame* 157 (4) (2010) 618–631.
[7] J. Li, Z. Zhao, A. Kazakov, et al., *Int. J. Chem. Kinet.* 39 (3) (2007) 109–136.
[8] G.P. Smith, D.M. Golden, M. Frenklach, et al., GRI-Mech 3.0, 1999. Available at http://www.me.berkeley.edu/gri_mech/.
[9] X.Q. You, T. Russi, A. Packard, et al., *Proc. Combust. Inst.* 33 (1) (2011) 509–516.
[10] A.S. Tomlin, *Proc. Combust. Inst.* 34 (2013) 159–176.
[11] T. Nagy, T. Turanyi, *Int. J. Chem. Kinet.* 43 (7) (2011) 359–378.
[12] M.T. Reagan, H.N. Najm, P.P. Pebay, et al., *Int. J. Chem. Kinet.* 37 (6) (2005) 368–382.
[13] M.T. Reagan, H.N. Najm, B.J. Debusschere, et al., *Combust. Theor. Model.* 8 (3) (2004) 607–632.
[14] M.T. Reagan, H.N. Najm, R.G. Ghanem, et al., *Combust. Flame* 132 (3) (2003) 545–555.
[15] D.A. Sheen, X.Q. You, H. Wang, et al., *Proc. Combust. Inst.* 32 (1) (2009) 535–542.
[16] D.A. Sheen, H. Wang, *Combust. Flame* 158 (12) (2011) 2358–2374.
[17] K. Braman, T.A. Oliver, V. Raman, *Combust. Theor. Model.* 17 (5) (2013) 858–887.
[18] R. Feeley, M. Frenklach, M. Onsum, et al., *J. Phys. Chem. A* 110 (21) (2006) 6803–6813.
[19] R. Feeley, P. Seiler, A. Packard, et al., *J. Phys. Chem. A* 108 (44) (2004) 9573–9583.
[20] M. Frenklach, *Proc. Combust. Inst.* 31 (1) (2007) 125–140.
[21] M. Frenklach, A. Packard, P. Seiler, in: Proceedings of the 2002 American Control Conference, 2002, pp. 4135–4140.
[22] M. Frenklach, A. Packard, P. Seiler, et al., *Int. J. Chem. Kinet.* 36 (1) (2004) 57–66.
[23] T. Russi, A. Packard, R. Feeley, et al., *J. Phys. Chem. A* 112 (12) (2008) 2579–2588.
[24] X.Q. You, A. Packard, M. Frenklach, *Int. J. Chem. Kinet.* 44 (2) (2012) 101–116.
[25] M. Frenklach, H. Wang, M.J. Rabinowitz, *Prog. Energy Combust. Sci.* 18 (1) (1992) 47–73.
[26] A.P. Kelley, A.J. Smallbone, D.L. Zhu, et al., *Proc. Combust. Inst.* 33 (2011) 963–970.
[27] F. Wu, A.P. Kelley, C.K. Law, *Combust. Flame* 159 (4) (2012) 1417–1425.
[28] J. Santner, F.M. Haas, Y. Ju, et al., *Combust. Flame* 161 (1) (2014) 147–153.
[29] F. Wu, Z. Chen, Y. Ju, et al., *Proc. Combust. Inst.* 35, 2015, accepted for .
[30] H. Sun, S.I. Yang, G. Jomaas, et al., *Proc. Combust. Inst.* 31 (1) (2007) 439–446.
[31] A. Burcat, B. Ruscis, <http://garfield.chem.elte.hu/Burcat/burcat.html>, (accessed 30.09.10).
[32] X.Q. You, H. Wang, E. Goos, et al., *J. Phys. Chem. A* 111 (19) (2007) 4031–4042.
[33] A.V. Joshi, H. Wang, *Int. J. Chem. Kinet.* 38 (1) (2006) 57–73.
[34] G.E.P. Box, W.G. Hunter, J.S. Hunter, *Statistics for Experimenters: An Introduction to Design, Data Analysis, and Model Building*, Wiley, New York, 1978.
[35] R.J. Kee, J.F. Grcar, M.D. Smooke, et al., PREMIX: A Fortran Program for Modeling Steady Laminar One-Dimensional Premixed Flames, Report No. SAND85-8240, Sandia National Laboratories, 1985.
[36] M. Frenklach, *Combust. Flame* 58 (1984) 69–72.
[37] T.J. Santner, B.J. Williams, W. Notz, *The Design and Analysis of Computer Experiments*, Springer, New York, 2003.